

FRAMATOME COGEMA FUELS

March 17, 2000
GR00-32.doc

U. S. Nuclear Regulatory Commission
ATTN: Document Control Desk
Washington, D. C. 20555

Reference: Stewart Bailey to T. A. Coleman, Request For Additional Information –
Framatome Topical Report BAW-10133P, Addendum 1, "Mark-C Fuel Assembly
LOCA-Seismic Analysis," Revision 1 (TAC No. M99906), January 4, 2000

Gentlemen:

Enclosed find the responses to the questions in the NRC request for additional information that was included with the reference letter. In accordance with 10 CFR 2.790, Framatome Cogema Fuels (FCF) requests that these responses be considered proprietary and withheld from public disclosure. An affidavit supporting this request is attached.

Attachment 1 is the FCF proprietary version of the responses. Attachment 2 is the affidavit identifying the criteria for the proprietary request. Attachment 3 is the non-proprietary version of the responses. These responses will be incorporated into the NRC-approved version of BAW-10133P, Addendum 1 as an appendix.

Should the staff reviewers have any additional questions or need any clarification on any of the responses, FCF would like to have a teleconference or meeting to discuss and resolve them.

Very truly yours,



T. A. Coleman, Vice President
Government Relations

cc: S. N. Bailey, NRC
J. Wermiel, NRC
S. L. Wu, NRC
M. S. Schoppman
R. N. Edwards
20A13 File/Records Management



Framatome Cogema Fuels

3315 Old Forest Road, P.O. Box 10935, Lynchburg, VA 24506-0935
Telephone: 804-832-3000 Fax: 804-832-3663

change: NRC PDC
1 10/10/00
TOUJ

Attachment 2

AFFIDAVIT OF THOMAS A. COLEMAN

- A. My name is Thomas A. Coleman. I am Vice President of Government Relations for Framatome Cogema Fuels (FCF). Therefore, I am authorized to execute this Affidavit.
- B. I am familiar with the criteria applied by FCF to determine whether certain information of FCF is proprietary and I am familiar with the procedures established within FCF to ensure the proper application of these criteria.
- C. In determining whether an FCF document is to be classified as proprietary information, an initial determination is made by the Unit Manager, who is responsible for originating the document, as to whether it falls within the criteria set forth in Paragraph D hereof. If the information falls within any one of these criteria, it is classified as proprietary by the originating Unit Manager. This initial determination is reviewed by the cognizant Section Manager. If the document is designated as proprietary, it is reviewed again by personnel and other management within FCF as designated by the Vice President of Government Relations to assure that the regulatory requirements of 10 CFR Section 2.790 are met.
- D. The following information is provided to demonstrate that the provisions of 10 CFR Section 2.790 of the Commission's regulations have been considered:
- (i) The information has been held in confidence by FCF. Copies of the document are clearly identified as proprietary. In addition, whenever FCF transmits the information to a customer, customer's agent, potential customer or regulatory agency, the transmittal requests the recipient to hold the information as proprietary. Also, in order to strictly limit any potential or actual customer's use of proprietary information, the substance of the following provision is included in all agreements entered into by FCF, and an equivalent version of the proprietary provision is included in all of FCF's proposals:

AFFIDAVIT OF THOMAS A. COLEMAN (Cont'd.)

"Any proprietary information concerning Company's or its Supplier's products or manufacturing processes which is so designated by Company or its Suppliers and disclosed to Purchaser incident to the performance of such contract shall remain the property of Company or its Suppliers and is disclosed in confidence, and Purchaser shall not publish or otherwise disclose it to others without the written approval of Company, and no rights, implied or otherwise, are granted to produce or have produced any products or to practice or cause to be practiced any manufacturing processes covered thereby.

Notwithstanding the above, Purchaser may provide the NRC or any other regulatory agency with any such proprietary information as the NRC or such other agency may require; provided, however, that Purchaser shall first give Company written notice of such proposed disclosure and Company shall have the right to amend such proprietary information so as to make it non-proprietary. In the event that Company cannot amend such proprietary information, Purchaser shall, prior to disclosing such information, use its best efforts to obtain a commitment from NRC or such other agency to have such information withheld from public inspection.

Company shall be given the right to participate in pursuit of such confidential treatment."

AFFIDAVIT OF THOMAS A. COLEMAN (Cont'd.)

- (ii) The following criteria are customarily applied by FCF in a rational decision process to determine whether the information should be classified as proprietary. Information may be classified as proprietary if one or more of the following criteria are met:
- a. Information reveals cost or price information, commercial strategies, production capabilities, or budget levels of FCF, its customers or suppliers.
 - b. The information reveals data or material concerning FCF research or development plans or programs of present or potential competitive advantage to FCF.
 - c. The use of the information by a competitor would decrease his expenditures, in time or resources, in designing, producing or marketing a similar product.
 - d. The information consists of test data or other similar data concerning a process, method or component, the application of which results in a competitive advantage to FCF.
 - e. The information reveals special aspects of a process, method, component or the like, the exclusive use of which results in a competitive advantage to FCF.
 - f. The information contains ideas for which patent protection may be sought.

AFFIDAVIT OF THOMAS A. COLEMAN (Cont'd.)

The document(s) listed on Exhibit "A", which is attached hereto and made a part hereof, has been evaluated in accordance with normal FCF procedures with respect to classification and has been found to contain information which falls within one or more of the criteria enumerated above. Exhibit "B", which is attached hereto and made a part hereof, specifically identifies the criteria applicable to the document(s) listed in Exhibit "A".

- (iii) The document(s) listed in Exhibit "A", which has been made available to the United States Nuclear Regulatory Commission was made available in confidence with a request that the document(s) and the information contained therein be withheld from public disclosure.
- (iv) The information is not available in the open literature and to the best of our knowledge is not known by Combustion Engineering, Siemens, General Electric, Westinghouse or other current or potential domestic or foreign competitors of Framatome Cogema Fuels.
- (v) Specific information with regard to whether public disclosure of the information is likely to cause harm to the competitive position of FCF, taking into account the value of the information to FCF; the amount of effort or money expended by FCF developing the information; and the ease or difficulty with which the information could be properly duplicated by others is given in Exhibit "B".

I have personally reviewed the document(s) listed on Exhibit "A" and have found that it is considered proprietary by FCF because it contains information which falls within one or more of the criteria enumerated in Paragraph D, and it is information which is customarily held in confidence and protected as proprietary information by FCF. This report comprises information utilized by FCF in its business which afford FCF an

AFFIDAVIT OF THOMAS A. COLEMAN (Cont'd.)

opportunity to obtain a competitive advantage over those who may wish to know or use the information contained in the document(s).



THOMAS A. COLEMAN

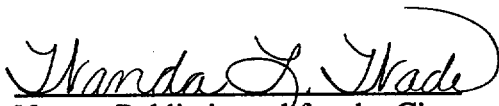
State of Virginia))
City of Lynchburg) SS. Lynchburg

Thomas A. Coleman, being duly sworn, on his oath deposes and says that he is the person who subscribed his name to the foregoing statement, and that the matters and facts set forth in the statement are true.



THOMAS A. COLEMAN

Subscribed and sworn before me
this 17th day of March 2000.



Notary Public in and for the City
of Lynchburg, State of Virginia.

My Commission Expires 8/31/01.

EXHIBITS A & B

EXHIBIT A

Responses to NRC Request for Additional Information on Topical Report
BAW-10133P, Addendum 1, "Mark-C Fuel Assembly LOCA-Seismic Analysis,"
Revision 1," January 4, 2000.

EXHIBIT B

The above listed document contains information which is considered Proprietary in
accordance with Criteria b, c, and d of the attached affidavit.

Attachment 3

RESPONSES TO NUCLEAR REGULATORY COMMISSION QUESTIONS ON
BAW-10133P, REVISION 1, ADDENDUM 1

1. Page 2-6, Section 2.2.2.4, states that damping increases significantly with increased axial flow. No data could be located in Addendum 1 for axial flow conditions used for damping investigations. Please provide any additional data that relates to the effect of axial flow on damping.

Response

The fuel assembly damping values were established from in water tests at conditions that simulated the complete range of reactor operating flow conditions. The effect of flow rate on the fuel assembly average percent critical damping derived from full-scale fuel assembly tests is shown in Figures Q1.1 and Q1.2. Figure Q1.1 was given in the original topical report BAW 10133PA, Rev. 1 (Figures 4.1 and 4.2 of Question 4).

Addendum 2 of BAW-10133P, Rev.1 was submitted to the NRC on May 17, 1999, which justifies the use of higher damping values in the fuel assembly seismic and LOCA models. All the relevant data for the use of higher damping values including Figures Q.1.1 and Q.1.2 are provided in the Addendum 2 report.

2. The bottom of page 2-7 states that the intermediate mass "m" is slightly greater than that of a grid "for numerical reasons." Please elaborate. Was this done for numerical stability?

Response

The use of a slightly greater mass than that of the actual grid results in the reduction of the mass of the assembly beam model. The overall mass of the assembly remains the same. The benefit of using a slightly higher mass is the improvement in the model run computation time. FCF has performed CASAC runs with actual grid mass [b,c,d], and no numerical instability problem was experienced. In fact, it was found in the analysis results that this change in the grid mass has no effect on the grid forces or on the model behavior.

CASAC uses an explicit numerical integration method. Effective stability is ensured by an automatic error control, which is usually kept significantly smaller than those required for impact description.

3. Appendix B gives some interesting results comparing the "hydrodynamic model" with the "masses added" model that was used previously. Were both of these models using the "newer" grid stiffness model? Please provide comparisons with the current model and the model that was previously used (i.e., without the

Addendum 1 modifications). Has it been shown that the new model bounds the data (i.e., over-predicts damage) including uncertainties in the data?

Response

All the test results presented in Appendix B were obtained by FRAMATOME. A comparison with test results using the "newer" grid model clearly shows that although the "hydrodynamic model" is effectively less conservative than the "mass added" model, the model results still remain notably conservative with respect to tests. It is shown in Appendix B of Addendum 1 (Figures B.5 and B.6) that the new model bounds the maximum in-water impact forces obtained from the fuel assembly seismic test programs for all level of seismic excitations (0.1 g to 0.6g). The influence of the coupling model has not been studied with the "older" grid model, yet it is very likely that similar trends would be obtained, since fluid coupling is exerted on the assembly lateral deformations, with no direct connection with the impact model at grid levels.

4. On page 3-1 (equation 3-3), the temperature scaling of equivalent damping makes use of temperature dependent stiffness (Young's modulus) ratios. Please explain the physical reason for this approach. Please substantiate the temperature independence of percent critical damping, or provide justification why this approach is adequately conservative.

Response

Single grid impact tests were performed at room temperature and at 600⁰F. The test results indicate that the temperature does not seem to affect the spacer grid structural damping, ζ_E .

In the pluck test with impact on grids which provides the equivalent impact parameters (K_{eq} , C_{eq}), the impact force signal is very similar to that of a single span mass M_{sp} impacting the equivalent stiffness K_{eq} . Then the spring-mass model of Section 3.2.2 is applicable. The calculation of the spring viscous damping is performed with the following relationship as given by Equation 3-1 in Addendum 1.

$$[b,c,d] \tag{1}$$

For the impact model, equivalent stiffness K_{eq} is corrected by the ratio of Young's modulus (hot and cold). Given the definition of the spring viscous damping (Equation 1) and as the spacer grid structural damping is not temperature dependent, the temperature scaling of the spring viscous damping leads to Equation 3-3 (viscous damping C_{eq} , proportional to the square root of K_{eq}) given on page 3-1 of Addendum 1.

More generally, the damping values associated with the impact stiffnesses do not have much influence as long as they remain within a reasonable range. In any

case, this influence is much smaller than that of the assembly damping introduced in the beam.

5. On page 3-3 (equation 3-6), the parameter Π is not defined. Please elaborate on the derivation of equation 3-6.

Response

The parameter not defined (Π) is the upper case of π (typographical error). This mathematical constant will be corrected in the final submission of Addendum 1. All the equations are derived from the response of the mass-spring-damper oscillator with initial zero deflection and initial velocity V_i . The impact ends when the net force in the spring-damper and therefore the mass acceleration vanish.

Equation 3-6 corresponds to the usual exponential damping factor:

$$[b,c,d]$$

where ω is the pulse of the undamped oscillator, and t is equal to the impact duration, such that :

$$[b,c,d]$$

which means that the impact duration is slightly shorter than a half-period. Equation 3-6 is approximate, but the approximation is quite satisfactory for small damping [b,c,d].

6. Page 2-6 states that alpha and beta are chosen in order to give the desired values of critical damping for the first mode and all higher modes. Please provide further justification for selecting the value of critical damping that was used for all higher modes.

Response

The damping values for the first and higher modes are provided in section 6 of Addendum 2 of BAW-10133P, Rev. 1. These values were obtained from the shaker modal tests, which were performed in air at room temperature. The damping values recorded were at very low amplitude. Based on the shaker table test results, the first mode and higher modes damping values are [b,c,d]. Therefore, using [b,c,d] damping value for the higher modes [b,c,d] is conservative.

The recent (November 1999) resonance tests performed at CEA in water under axial flow conditions on the Framatome fuel assembly clearly show that [b,c,d] damping (at least) for the higher modes is justified. This data is still in the process of documentation.

It may also be noted that in accident studies, there is less impact of the damping value for higher modes than for the first one. Effectively, the first mode is predominant in the seismic response. For the LOCA response, the contribution of higher modes is enhanced but the influence of damping is notably minimized in this very short transient, without sustained oscillations.

7. From the data on Table 4-1, it appears that fuel mass was considered in your model (by increasing the density of beam material), but fuel stiffness was neglected. This lack of fuel stiffness consideration appears to be the primary reason for requiring rotational stiffness elements at the beam nodes in order to match experimental results. Please explain why this approach is valid for all intended uses of this methodology.

Response

In lateral deformation, the fuel assembly behavior exhibits a high-shear effect, i.e. the modal frequencies are close to integer multiples of the first one. This results from an individual bending of all the tubes (fuel rods, guide-thimbles and instrument thimble), restrained in grids which remain almost horizontal, i.e. their rotations are much smaller than in a global beam bending, in which they would remain perpendicular to the neutral axis.

A completely phenomenological modelling of such a behavior is not accessible to a single beam model, which implies that the parameters must be adjusted to match the experimental frequencies. However, there exist relationships with the described behavior. In particular :

- the cross-sectional inertia is the sum of those of the guide-thimbles and fuel rod claddings, without any supplementary term allowing for the distance to the neutral axis,
- the initial values of the rotational stiffnesses are related to the rod restraining conditions, and the connection of the springs to a fixed node provides a restriction to the absolute rotation of the grids, i.e. with respect to the horizontal.

Increasing Young's modulus is not equivalent to the rotational springs, since it involves increasing in the same ratio frequencies corresponding to a predominant flexion, with little shear. An alternative solution which proves acceptable is to increase the cross-sectional inertia while using an artificially small shear area in Timoshenko's beam formulation, but the model presented in Addendum 1 is more physical.

The density of the fuel assembly provided in Table 4-1 is calculated by dividing the fuel assembly mass by the fuel assembly volume. The fuel assembly length is taken as the nozzle to nozzle guide tube length.

Benchmarking of the fuel assembly modeling in air remains unchanged from the previous modeling (section 2.2.1 of Addendum 1). In this part of the modeling,

the fuel assembly natural frequencies and lateral stiffness are benchmarked to the test results. To match the natural frequencies and lateral stiffness of the benchmark test, the rotational spring stiffness of the intermediate spacer grids are varied.

8. Please provide examples of licensing analyses of seismic and LOCA models for "limiting plant cases" comparing the new and old models.

Response

The maximum impact forces for "limiting seismic and LOCA time histories" generated by the new and old models are provided below. The input motion for the time histories as discussed in section 4 of BAW-10133P, Rev.1, Addendum 1 is given at the upper core plate, lower core plate, and upper baffle plate locations. The time duration of the analyses is [b,c,d] seconds for the seismic run and [b,c,d] second for the LOCA run. Three faulted conditions listed below were investigated.

It can be seen that the maximum impact forces generated by the new model are lower during the seismic event because of the incorporation of the hydrodynamic coupling and the new grid impact model into the core model. The impact forces generated by the new model during a LOCA, in two out of four faulted cases, are higher compared to the old model. From these results, it can be seen that incorporation of the hydrodynamic coupling has a strong effect on the fuel assembly seismic response (the total duration of the analysis is [b,c,d] seconds), and a small effect on the fuel assembly LOCA response (the total duration of the analysis is [b,c,d] seconds). The grid impact model used in the new model is consistent with that presently used by other fuel vendors.

b,c,d

Load Cases

SSE-X – Safe Shutdown Earthquake –X Direction
SSE-Z – Safe Shutdown Earthquake –Z Direction
SLB-X – Surge Line Break – X Direction
SLB-Z – Surge Line Break – Z Direction
SILB-X – Safety Injection Line Break – X Direction
SILB-Z – Safety Injection Line Break – Z Direction

9. The model described in B&W report BAW-10133PA was executed using the STARS code (1972, Ref. 1 of BAW-10133PA). The models described in the Addendum being reviewed are executed with the CASAC code (1996, Ref. 3 of BAW-10133P Addendum 1). Appendix A mentions that the CASAC code has been benchmarked against other finite element codes and closed form solutions. Are there issues with numerical instability, as discussed in Question 2 above, that result from use of the CASAC code? Please provide a copy of this verification report and provide justification that the switch in code usage does not require further review.

Response

Effective stability is ensured by CASAC as discussed in the response to Question 2.

[b,c,d]

The CASAC code has been extensively used by analysts at Framatome. All CASAC results are based on classical engineering concepts. In all test cases, very good agreements between the results of CASAC with exact form solutions or with the ANSYS results were found. (ANSYS is a widely used general purpose finite element program.)

The CASAC code has also been verified based on fuel assembly lateral pluck and impact test results.

The CASAC code has been certified by FCF in accordance with NRC-approved QA procedures.

10. References 5 and 9 of Addendum 1 were reviewed to gain background into the hydrodynamic coupling model. Flow models used in arriving at mass added parameters assume inviscid, irrotational, two-dimensional flow. It appears that the same flow model is used to arrive at "masses" regardless of node elevation. Please provide justification that this is suitable for nodes near the assembly ends.

Response

The reviewer's interpretation is correct that the same fluid model is used to arrive at "masses" regardless of node elevation, since this model is based on the two-dimensional flow hypothesis with a uniform flow pattern along the fuel assemblies. The two-dimensional flow hypothesis is based on the highly extended character of the structures, with lateral motions only (i.e. beam modeling), and negligible end effects.

The latter hypothesis is not specific to the proposed coupling model. It is implicit in the commonly used added mass model, in which the in-water frequency decrease observed in out-of-core tests is merely reflected by a uniformly increased beam mass.

For PWR fuel assemblies, negligible end effects are justified by the effectively very slender character of the structures, and more especially, since the most significant scaling length for the fluid flow is the rod pitch. (A good approximation of coupling is obtained with a model of a single rod cell as described in section 3.3 of Reference 10 of Addendum 1). In addition, coupling has no influence on the motions at assembly ends, which are input. For comparison, fuel storage racks in a pool are much less slender, and the rack tops are free to move next to a plenum, which leads to a significant vertical fluid motion and coupling decrease (see additional Reference 1A of this document-Enclosure 2).

11. Page 2-6 gives non-dimensional values for the assembly added mass and the coupling with baffles for a 17X17 assembly, and states the values are "derived from a fluid model." While these values are similar to those reported in Reference 10 of Addendum 1, no detail of the fluid model was given. Please provide details of the fluid model.

Response

The fluid model and its description are provided in Reference 1A of this document. Figure Q11.1 represents the schematic of this model, which comprises of a 3x3 array of 9x9 rod array assemblies. Figure Q11.2 represents the fluid mesh, reduced to the lower right quarter from symmetries with respect to the X and Y axes. As reported in Reference 10 of Addendum 1, the rod diameter – [b,c,d] and pitch [b,c,d] correspond to the 17x17 design. Gaps of [b,c,d] between assemblies or with the core baffles are included (average in-core value).

For the determination of the added mass term m_a , the lateral confinement of the rows along the motion direction X is obtained by accelerating simultaneously the center assemblies in the rows along X, i.e. the complete central row along Y. The

coupling term with the baffles m_c is not dependent on any hypothesis on the assembly motions, since it can be obtained from the baffle acceleration.

The dimensionless values of m_a and m_c are respectively equal to [b,c,d] and [b,c,d] for the assembly in center position. The sum is not exactly equal to [b,c,d], and the [b,c,d] difference reflects the small coupling with other assemblies. The calculated values are rounded-off and very slightly modified to fulfill exactly the consistency relationship, thus yielding the structural model values [b,c,d] and [b,c,d]. The very small decrease in absolute value with respect to those in Ref. 10 mainly results from the gap between assemblies.

Further details and analyses are given in Reference 1A.

12. It is the reviewers understanding (from reviewing Ref.10 of Addendum 1) that :
- a. The fluid coupling masses added to the assembly nodes were independent of assembly position in the model, and varied with grid number (Table 4-1) because of the differences in element lengths (as specified in 4.3.6). Please elaborate if this interpretation is not correct.
 - b. Hydrodynamic coupling "between" assemblies was totally neglected. Please elaborate if this interpretation is not correct.

Response

The interpretations are absolutely correct.

Additional Reference :

- 1A RIGAUDEAU, J., Hydrodynamic Coupling in Seismic Response of PWR Fuel Assemblies and Other Immersed Structures, ASME-PVP Conference, Boston 1999, PVP-Vol. 394.

[b,c,d]

**Figure Q1.1 FCF Mark-C 17 x 17 FA
Average First Cycle Damping Under
Flowing Conditions**

[b,c,d]

**Figure Q1.2 Damping Versus Effective
Amplitude of Displacement**

[b,c,d]

**Figure Q11.1 Schematic of the Fluid Model
Of a 3 X 3 Assembly Array**

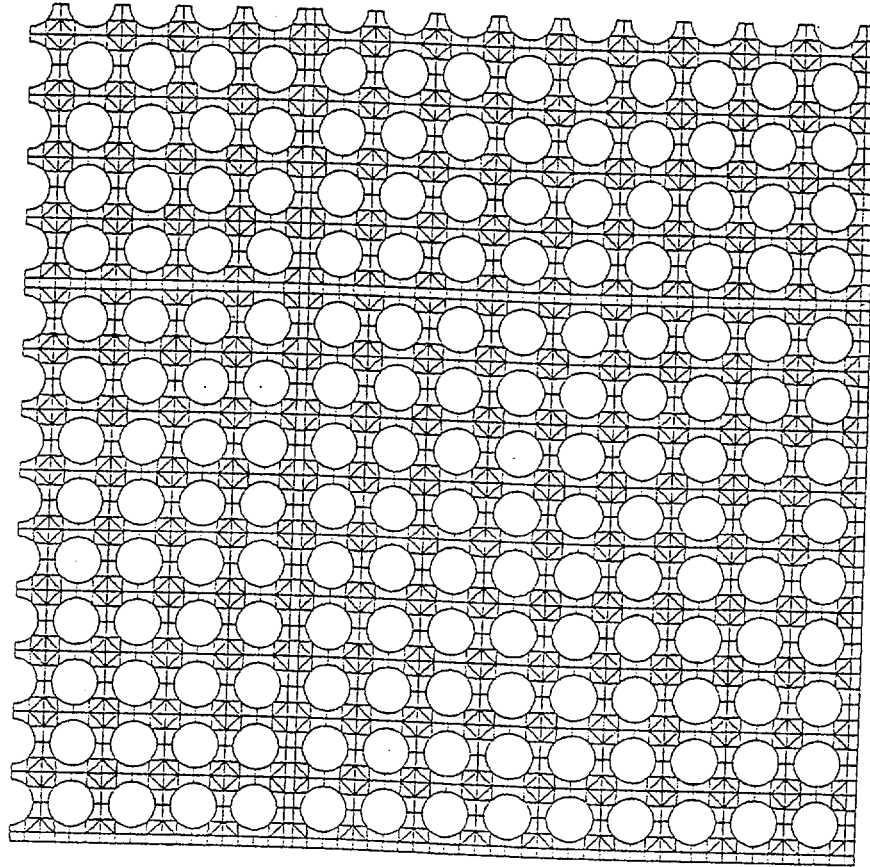


**Figure Q11.2 Fluid Model of the
3 x 3 Assembly Array**

Enclosure 1

[b,c,d]

Enclosure 2

PVP Conference Paper on Fuel Assembly Fluid
Model

HYDRODYNAMIC COUPLING IN SEISMIC RESPONSE OF PWR FUEL ASSEMBLIES AND OTHER IMMERSSED STRUCTURES

Jean Rigau
FRAMATOME Nuclear Fuel
10, rue Juliette Récamier
69456 LYON Cedex 06, France
Phone : 33 4 72 74 88 37
Fax : 33 4 72 74 88 08
e-mail : jrigau@framatome.fr

ABSTRACT

The influence of hydrodynamic coupling is not negligible in the seismic response of immersed structures, such as PWR fuel assemblies. The coupling basic features are first presented as guidelines to consistent modelling, in which the fluid containment plays an essential part. Finite element solutions are applied to plane coupling between highly extended structures. For the assembly single row model currently used in core seismic analysis, a coupling model based on the row lateral confinement proves very simple, and justified from calculations and tests. The case of fuel storage racks is considered for comparison and appears to be more complex for applications. Non linear effects are briefly discussed.

1. INTRODUCTION

In the response of PWR fuel assemblies to horizontal seismic loads, the influence of primary coolant is far from negligible. Unlike fluid-induced damping which is currently included in structural damping, allowance for the non-dissipative hydrodynamic coupling requires specific elements in the structural model. The aim of the paper is to show how a realistic and readily applicable model can be obtained from appropriate assumptions and calculations. The case of fuel storage racks is also considered but less extensively, in order to display the differences and similarities encountered in the coupling properties for various kinds of immersed structures. Except when otherwise stated, coupling is assumed linear, and the structures are considered as highly extended with perfectly rigid cross-sections (beam modelling), which leads to plane fluid models for coupling estimate. A typical description of such a coupling is given by Fritz (1972).

2. COUPLING FUNDAMENTAL FEATURES AND DETERMINATION

2.1. General equations and coupling effect

By assuming small motion amplitudes in an incompressible and

non-viscous fluid, continuity and momentum transfer equations are linearized :

$$\text{div } \vec{V} = 0 \quad (1)$$

$$\text{grad } P = -\rho \frac{\partial \vec{V}}{\partial t} \quad (2)$$

where V , P and ρ stand for fluid velocity, pressure and density respectively. Therefore the pressure field is a solution of Laplace equation :

$$\Delta P = 0 \quad (3)$$

with boundary conditions corresponding to the structural acceleration component perpendicular to the solid surface (through eq. (2)). Coupling then results from the reciprocal action of pressure loads on structural motions, and for discrete models, the linear force-acceleration relationship leads to the well known added mass matrix concept :

$$F_{\text{hydrodynamic}} = -M_A \ddot{X} \quad (4)$$

where X is the structural displacement vector. For rigid structures and a single direction for motion and forces, each matrix term is defined by the resultant of pressure forces ($-m_{ij}$) on structure S_i generated by a unit acceleration of S_j , and vice-versa.

2.2. Physical interpretation

The fluid motion is entirely governed by continuity and may be considered from a purely kinematic standpoint. From linearity and commutativity of the space and time derivatives, the motion can be represented by the displacement, velocity or acceleration fields, all satisfying the continuity equation (1), with the corresponding potentials as solutions of Laplace equation (3). Advanced finite element formulations use the displacement potential for symmetry considerations

in generalized forms as described by Jeanpierre et al. (1979). Continuity macroscopic balances performed on velocity allow approximate solutions by applying Lagrange equations to the fluid kinetic energy, as presented by Scavuzzo et al. (1979) for rectangular shapes. Yet from a dynamic standpoint, acceleration is the only significant field since producing the resultant pressure forces through the pressure gradient (2). These forces are directly related to the magnitude of acceleration along the structures, unlike in the steady flow where the pressure gradient is related to that of velocity, and leads to zero forces on submerged bodies in an ideal fluid (d'Alembert's paradox).

Conversely, the non-stationary character is obvious from the added mass matrix representation, but the fluid kinematics should not be neglected. The concept of inertia is valid indeed for a fluid particle, or for global effects from the supplementary fluid kinetic energy : positive definite matrix and frequency decrease, sum of the matrix terms for one direction equal to the fluid mass (when completely bounded by the structures). But as the coupling terms individually represent hydrodynamic forces, they may be negative (when non-diagonal) and depend on the direction; above all, under confined conditions, they may become large with respect to the fluid mass, merely because in out-of-phase motions, the fluid acceleration is large when compared with the structural ones.

2.3. Consistency relationships for sets of immersed structures

Consider a set of (n - 1) immersed solids S_i , with S_n corresponding to the containment, and a rigid-body acceleration (γ) of such a system. Then fluid acceleration and pressure gradient are uniform, and eq. (2) is very similar to that of hydrostatics; this implies that the resulting force on S_i is equal to ($m_{di}\gamma$), where m_{di} stands for the displaced fluid mass used in buoyancy force ($m_{di}g$). For the containment, the force is opposite, with a mass corresponding to the internal volume completely filled with fluid. Hence the consistency relationships are derived :

$$\sum_{j=1}^n m_{ij} = -m_{di} \quad i = 1 \text{ to } (n - 1) \quad (5a)$$

$$\sum_{j=1}^n m_{nj} = +m_{dn} \quad (5b)$$

Then the total sum of m_{ij} 's is equal to the fluid mass, yet this mass merely represents the fluid inertia, although the displaced masses m_{di} are typical of a fluid problem. Moreover, when considering a non-rigid but forced (or quasi-static) structural response, the relative accelerations are negligible, and the response of S_i is proportional to the loading force :

$$f_i(t) = -(m_i - m_{di})\gamma(t) \quad (6)$$

where m_i stands for the solid mass. Coupling then leads to a decrease in loading inertia forces for immersed structures, instead of a fictitious increase when allowing for a single added mass m_{di} only. This physical interpretation of consistency relationships (5) in a particular but realistic case clearly calls for their fulfilment in coupling models.

Equations (5) are generally known for the two-body problem, i.e. "nested" bodies separated by the fluid; they have been established by Fritz (1972), and applied by Scavuzzo et al. (1979) to consistent coupling determination from the single estimate of the added mass at the

inner structure (hydrodynamic mass). However, they are more often ignored for larger sets of structures, since the greater complexity requires assumptions and simplifications which may prove inadequate. A single added mass at the fuel assemblies is used in many PWR core models, neither consistent nor reflecting the in-core confinement since determined from out-of-core frequency tests. Another typical trend is to include effective coupling between neighbouring structures, but to neglect it when structures are remote or shielded by other ones. This may be quite acceptable for coupling between the immersed structures, certainly not with the containment whose acceleration generates a non-negligible pressure gradient everywhere inside.

2.4. Finite element solution and input in structural models

A finite element (f.e.) determination of the added mass matrix for coupling between rigid outlines has been described by Levy and Wilkinson (1975), but has not been found available in standard f.e. programs, where coupling is defined for deformable structures. Yet this method can easily be derived from the mathematically equivalent and widely used thermal formulation. When representing pressure by temperature, acceleration by the heat flux, the fluid matrix H to be solved is identical to the thermal one with conductivity $k = 1/\rho$. The loading vectors Q discretizing the unit acceleration of the different structures are defined such that $Q^T P$ represents the resultant of pressure forces. Hence :

$$m_{ij} = Q_i^T H^{-1} Q_j \quad (7)$$

whose perfectly symmetric feature is typical of the coupling variational formulations.

This method is implemented in the f.e. program SYSNUKE, designed for thermo-mechanical calculations in the nuclear industry. The determination of the complete two-dimensional coupling is possible, including the cross-directional XY terms. Graphical interactive facilities allow easy modelling, and the visualization of the fluid acceleration field (much more convenient than iso-pressure lines) is directly feasible since already available for the heat flux. Quadratic elements are well suited for representing the rod circular outlines and permit a relatively coarse meshing, as verified from comparison with the analytical solution for co-axial cylinders.

The plane coupling f.e. models yield values per unit height, and in the structural models, coupling is considered only between nodes at the same vertical level; the values are proportional to the modelled height (similarly to the structural mass of beams), and input in the elements coupling two nodes.

2.5. Dimensionless coefficients

Except when comparing with the structural mass, all the numerical values given hereafter are in the commonly used dimensionless form, as the ratio of the coupling term to the displaced fluid mass. This implies a right hand side equal to -1 in eq. (5a) for the immersed structures. For sets of identical structures, there is a single reference mass, and comparison is possible between all the coupling terms, except for the added mass at the containment (not considered here since the containment motion is assumed to be an input). For fuel assemblies, direct comparison is possible between different rod array sizes, including a single rod.

3. BASIC MODEL FOR A FUEL ASSEMBLY ROW

3.1. Lateral confinement hypothesis and resulting fluid models

PWR fuel assemblies are tall and laterally flexible structures only restrained at their ends by the horizontal core plates. Horizontal seismic loads then produce fuel assembly lateral distortions, and impacts between the latter or with the core vertical baffles; such impacts are located at the grids restraining the fuel rods. The current models used for the justification of fuel assembly lateral strength comprise a fuel assembly single row, excited in its own direction X, in which the assemblies are represented by beams, and springs with gaps for impacts (Callens et al., 1991).

The implicitly assumed mechanical independence of such rows can be extended to coupling by considering that the modelled row is laterally confined. Also assuming negligible gaps between rows, it has been demonstrated by Rigaudeau et al. (1993) that the lateral confinement is equivalent to identical motions of the rows and also that coupling can be determined in a fuel rod single row, parallel to the motion direction X. In the previous reference, the fluid model represents 3 "assemblies", each comprising 3 fuel rods, then allowing for inner or edge positions of assemblies and rods; in-row gaps between assemblies and with the baffles are included.

3.2. Coupling features

The coupling features corresponding to the lateral confinement are the following :

- coupling between assemblies is negligible,
- the remaining terms, i.e. the added mass m_a at assembly (hydrodynamic mass) and the coupling term m_c with the core baffles, are independent of assembly position,
- the fuel rod contributions to coupling are almost identical, which allows easy extrapolation to a full-scale rod bundle.

The numerical results from the rod single row model are given in table 1, for the 17 x 17 rod array design in which the fuel rod diameter and pitch values are 9.5 mm and 12.6 mm respectively. The fulfilment of the consistency relationship by $(m_a + m_c)$ is achieved to within a -0,001 difference, corresponding to the very small negative coupling between neighbouring assemblies.

Table 1. Coupling coefficients from the rod single row model

	Ratio to displaced fluid mass m_d	Ratio to solid mass PWR conditions
Added mass m_a	2.675	0.253
Baffle coupling m_c	- 3.674	- 0.348
$m_a + m_c = m_d$	- 0.999	- 0.095

The coupling model finally reduces to a two-body one, the same for all the assemblies. Consider an immersed beam (assembly), supported and excited by the containment (core plates and baffles) with acceleration $\gamma(t)$. As the coupling linear distribution along the beam is similar to that of structural mass m , the relative lateral displacement x of any node with associated height h is given by the equation :

$$h(\bar{m} + \bar{m}_a) \ddot{x} + (\text{other terms}) = -h(\bar{m} - \bar{m}_d) \gamma(t) \quad (8)$$

where over-lining refers to values per unit height and the "other terms" depend on the beam stiffness and damping properties. Therefore the loading force decrease resulting from the extension of Archimede's principle (eq. (6)) applies to the beam response even when dynamic (and obviously to the response of a mass-spring system). If the frequency reduction from added mass has a limited effect on the spectrum value for the first beam mode, predominant in linear response, then this response should also be decreased by the coupling effect. Yet for the in-core seismic behaviour of the fuel assemblies, strongly non-linear because of the many impacts, the influence of coupling can be estimated only from time-history calculations, and tests (paragraph 5.2).

The somewhat surprising features of the previous coupling model can be interpreted from fluid continuity with lateral confinement, as by Rigaudeau et al. (1993) for the rod single row, and below in the more elaborate models which are precisely designed for an analytical estimate of the hypothesis validity.

4. FUEL ASSEMBLY ARRAY ANALYSIS

4.1. Model description

Figure 1 represents the fluid mesh of a 3 x 3 array of 9 x 9 rod array assemblies, reduced to one quarter from symmetries and then comprising 9000 nodes. As in section 3, the rod diameter and pitch correspond to the 17 x 17 design; the 2 mm value of gaps between assemblies or with baffles is the average in-core value. The single X direction of assembly motions is considered, to which relative positions are referred : "axial" in the X direction, "lateral" in the perpendicular Y direction.

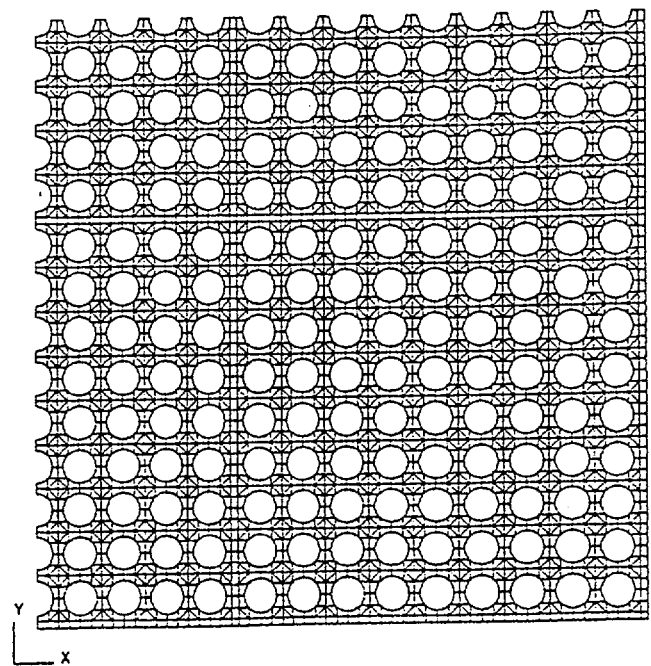


Figure 1 : Fluid model of the 3 x 3 assembly array

The motion field is skew-symmetric with respect to the symmetry axis along Y, which is represented by the boundary condition $P = 0$ on this axis. It is noteworthy that with the symmetry reduction, the acceleration of a single structure is possible only if the structure contains both symmetry axes (center assembly or baffles); otherwise, the non-represented symmetric structure(s) is (are) also accelerated. A complementary model of a single 9×9 assembly (one quarter from symmetries) allows the specific influence of lateral gaps to be studied, from zero to 35 mm values, with a 35 mm axial gap.

4.2. Restriction to identical assembly row motions

From the symmetry properties, the acceleration of all the middle assemblies in rows along X is performed, thus corresponding to identical motions of such rows. Baffles are also accelerated for a check and the acceleration visualization. Table 2 displays the m_a and m_c values for the accelerated assemblies, and when obtained from the single assembly model. Without lateral gap in the single assembly model, the values are very close to those in table 1, which are therefore confirmed for a strict lateral confinement. In the other cases, the influence of the small lateral gaps is also small but not completely negligible, thus illustrating the result sensitiveness to the lateral confinement conditions.

The fulfilment of the consistency relationship by $(m_a + m_c)$ is (evidently) rigorous for the single assembly; in the assembly array, the differences still reflect the negligible axial coupling between assemblies, although larger than in the rod single row model because of the lateral gaps.

Table 2 : Coupling coefficients from the single assembly model and from the assembly array model.

	Added mass m_a	Baffle coupling m_c	$m_a + m_c$
Single assembly, no lateral gap	2.689	- 3.689	- 1.000
Single assembly, 2 mm lateral gap	2.489	- 3.489	- 1.000
Assembly array, center position	2.563	- 3.543	- 0.980
Assembly array, flank position	2.540	- 3.535	- 0.995

The acceleration field patterns are shown on figures 2 and 3, in the center assembly and the neighbouring regions. Such patterns are related to the acceleration flux conservation, with "sources" on accelerated outlines only, and to the existence of lateral confinement.

When accelerating all the middle assemblies in rows along X, the field cannot spread outside, where there are no flux sources, and the fluid motion is located around the accelerated rods. This leads to a very weak or zero pressure gradient in other assemblies, and therefore coupling is negligible with these assemblies; but the pressure difference generated between the accelerated assembly ends is completely transferred to the baffles, at any distance. As most of the fuel rod generated flux is transferred from one rod side to the other, there results approximate independence of fuel rod cells and therefore similar fuel rod contributions. The uniform character of coupling with baffles is still

more obvious for baffle acceleration : the field appears to be space-periodic, just because the fluxes at cell boundaries are identical to the flux generated on baffles. This feature is confirmed by the uniform field in gaps along X, and moreover in the large axial gap of the single assembly model (figure 4), which displays the negligible influence of axial gaps in laterally confined models.

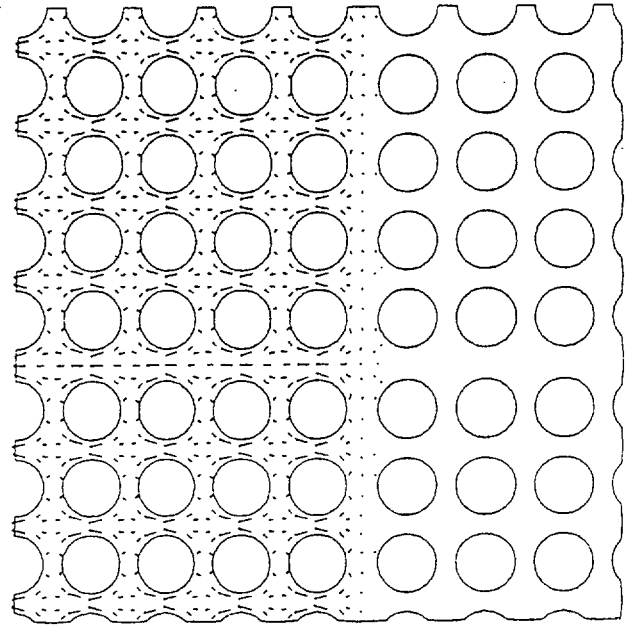


Figure 2 : Acceleration of middle assemblies in array

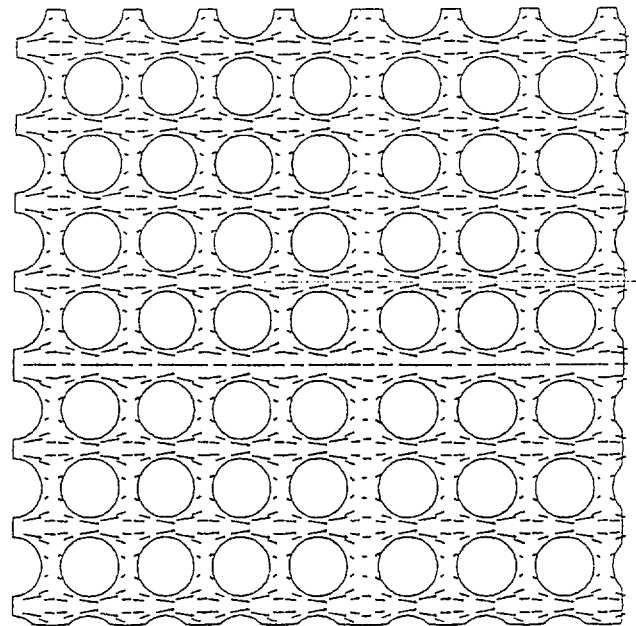


Figure 3 : Baffle acceleration in assembly array

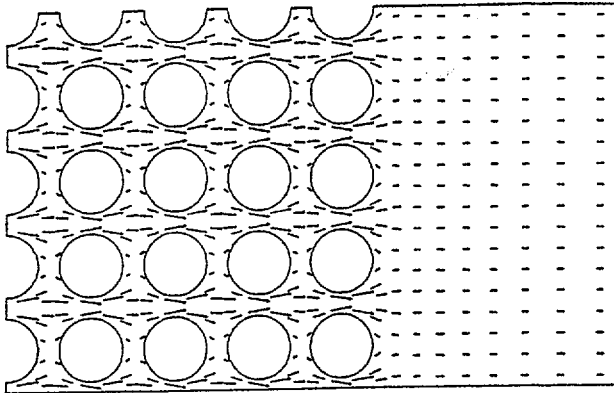


Figure 4 : Baffle acceleration in single assembly model

The approximate independence of the rod cells is confirmed by a single rod model, with baffles at cell boundaries, which yields coupling terms larger than the previous ones (without lateral gaps) by less than 10 %. It is noticeable that this property is obtained for a relatively small pitch/diameter ratio, therefore a dense array, since it is obvious only for tiny rods in wide cells, with much smaller coupling ($m_a = 1$ and $m_c = -2$ for cylinders in a large plenum). This provides a justification for the homogenization methods such as described by Brochard and Hammami (1991), which are also particularly suited to the large but confined tube bundles in steam generators.

4.3. Coupling distribution for any motion

Acceleration of the center assembly provides all the coupling terms relating to this assembly. For a more visual representation, table 3 displays the results in a geometrical configuration reproducing that of the complete 3 x 3 array, with baffles on the right : each division yields the coupling between the corresponding assembly (or baffles) and the center one, whose added mass is in the center division (1.608).

Coupling with baffles is identical to that in table 2 for the same center assembly since it may represent just as well the forces exerted on motionless assemblies resulting from baffle acceleration. Coupling between assemblies appears to be very moderate, in particular with diagonal positions, or even with axial positions and therefore in the rows along X used in seismic calculations. The more notable reduction in added mass is directly related to the larger lateral coupling terms, since from coupling linearity and symmetry, addition with these terms (sum in the table middle column) leads to the former 2.563 value.

Table 3 : Geometrical representation of coupling coefficients with the center assembly, in the assembly array.

0.093	0.477	0.093	- 3.543 (baffles)
- 0.196	1.608	- 0.196	
0.093	0.477	0.093	

Without lateral confinement of the accelerated assembly, the acceleration field can spread outside (figure 5) with a pattern comparable to that in the single assembly model with a 35 mm lateral gap, for which the added mass is 1.515. The field decrease with distance, from flux conservation, is such that inter-assembly coupling remains moderate. Inside, balance with external flux requires a flux transfer and then a pressure gradient between the rod cells, opposing that around the rods and leading to the added mass decrease. The field patterns around different accelerated rods are no longer identical but remain similar, the rod added mass ranging from 1.330 to 1.936 (along the lateral and axial gap respectively), the 1.608 overall value being obtained for the central rod. Also, it is noteworthy that the assembly coupling configuration is comparable to that between individual rods. Such results are favourable to the representative character of the model size, and to the homogenization method mentioned above.

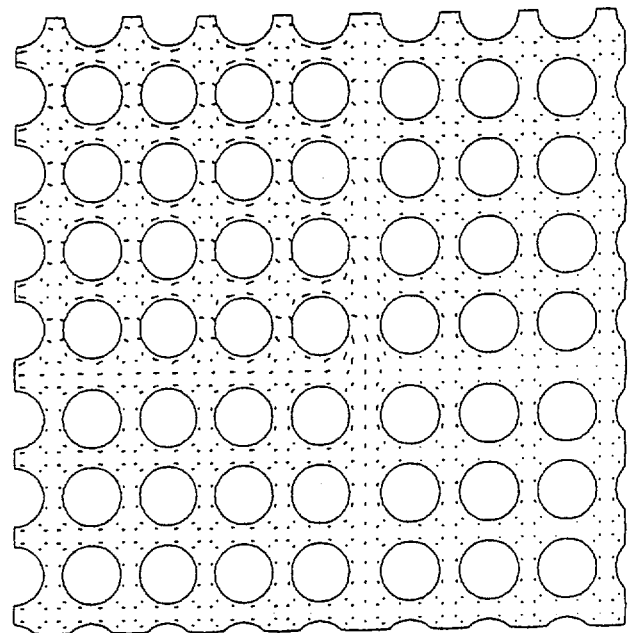


Figure 5 : Acceleration of center assembly in array

4.4. Analytical justification of the basic model

The previous results for any motion are hardly applicable to the assembly single row structural model, since the in-row coupling terms are not consistent without out-of-row coupling. Using the added mass from table 3 in the two-body basic model would lead to $(m_a + m_c)$ equal to - 1.934 instead of -1, and therefore to a decrease in loading forces twice as large as the physical one. This non-conservative trend is enhanced when introducing the negative coupling terms between assemblies, which are also far too weak to have any significant influence on assembly differential motions and impacts. Neither is the development of a complete core model justified only for introducing coupling between assemblies, much smaller than with baffles.

5. FUEL ASSEMBLY SEISMIC TESTS AND CALCULATIONS

5.1. Test program

Shaker table tests on sets of interacting fuel assembly mock-ups have been undertaken in cooperation with the Commissariat à l'Energie Atomique (C.E.A.). Detailed test description and results are presented by Queval et al. (1991, 1993), and Leroux et al. (1993). The mock-ups can be arranged either in a single row (5 or 13 mock-ups) or in a reduced scale core configuration (5 mock-ups in the longest rows), with bi-axial excitation in the latter case. Tests are performed in air or in water, with a confinement simulating the core baffles, and using accelerograms generated from a seismic design basis spectrum.

The mock-up design is based on a reduced 6 x 6 fuel rod array, but with rod diameter, pitch and restraining conditions typical of the 17 x 17 design. Then the mock-up behaviour proves similar to that of a scale 1 assembly in characterization tests, i.e. single assembly lateral response without or with impacts at grid levels. The mock-up row model is built with the same procedure as for seismic analysis of scale 1 assemblies. Coupling is allowed for by the basic model previously presented, also using for comparison a single added mass at assembly, which is determined from experiments with little confinement ($m_{14} = 1.25$). The in-water increase in damping is found relatively small from characterization tests, and therefore should not screen the influence of coupling when introduced in the model.

5.2. Main results and consequences

For the assembly single row model representativity, one of the most important results is certainly the similar behaviour of a laterally confined row and of the longest rows in the core configuration. On figure 6, the maximum in-water impact forces, at the row ends, appear to be coherent when considering the natural scatter of such forces, which are dependent on the precise impact sequence and on the non-uniform gap distribution in the rows (gaps are uniform in the models since the actual in-core gaps are unknown). The model is found conservative, yet significantly less with the consistent coupling model than with the single added mass.

Another typical feature reflected by tests and calculations is the existence of an approximately in-phase overall motion of assemblies, between the main impact sequences which occur in assembly clusters when blocked by the baffles. As a result, coupling can be assumed as mainly exerting on a similar motion of all assemblies, which includes the basic assumption of identical row motions.

The model qualification is performed on the 13 mock-up row, in which the impact forces are larger. Figure 7 presents the in-air and in-water maximum impact forces, as an average on the 4 grids withstanding the largest forces (the two grids near mid-assembly, at both row ends). The model is still conservative, yet the consistent coupling model leads to a force decrease which is consistent with the test results, but not reflected with the single added mass. Similar trends are observed on other response parameters (force integral, number of impacts and total duration in the time-history).

Obviously, a complete and accurate validation of the coupling model is hardly feasible, due to the approximate character of the structural model, and to the complex phenomena to be described, also noting that in fuel assembly response, coupling remains a corrective term even if significant. Under such conditions, the coupling model is justified from its global coherence with the observed effects, to within

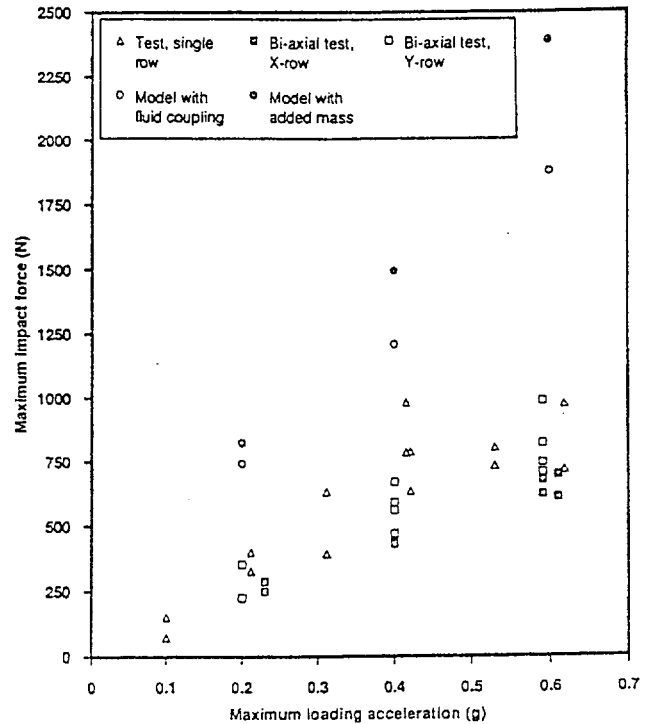


Figure 6 : Impact forces for in-water 5-mock-up rows

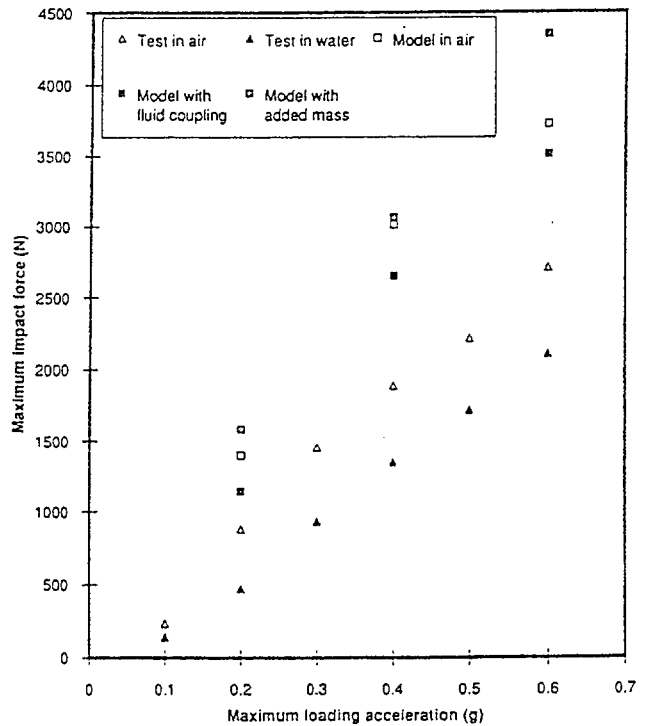


Figure 7 : Impact forces in the 13-mock-up row

the modelling uncertainties. Moreover, the model conservatism is mainly related to the impact description, much more difficult than that of assembly lateral deformations; this means that a conservatism margin reduction from the impact modelling can be envisaged only with caution, which precisely implies the elimination of clearly identified conservatisms from non-consistent coupling models.

6. FUEL STORAGE RACKS

6.1. Configuration and fluid modelling

PWR spent fuel storage racks consist of an array of rectangular modules, free-standing in a pool and comprising cells in which the fuel assemblies are inserted. The fluid mesh on figure 8 corresponds to the layout of a configuration which is simple but sufficiently representative for illustrating most of the coupling properties. The single X direction of rack motions is considered, along the longest 3-rack rows, for coupling between racks or with the pool walls only. The basic model for in-core coupling is obviously applicable to the fuel-to-cell coupling but allowing for slightly larger gaps.

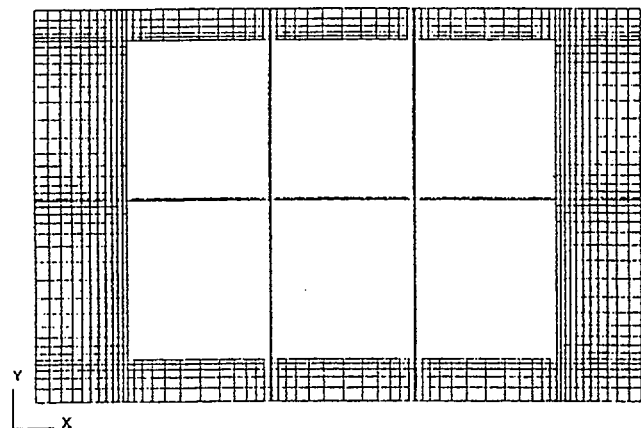


Figure 8 : Fluid model of racks in the pool

The horizontal dimensions are 12.6 m x 8 m for the pool, 2.96 m x 3.24 m for the racks, with a 34 mm gap between racks. The rack array off-centering in the Y direction is 110 mm which is little significant in coupling values. The results are given only for coupling with racks located in the row neighbouring the smaller gap with pool wall.

As the total water depth is 12 m, and the rack height is 4.43 m, the depth over the racks is large enough for neglecting the interaction with sloshing, also considering that the first sloshing frequencies are extremely small (0.25 Hz along X). However, due to the existence of the large water plenum, together with racks less slender than fuel assemblies, the coupling reduction from the vertical fluid motion is not negligible and will be briefly discussed.

6.2. Result analysis

Table 4 displays the coupling terms with the same geometrical representation as in table 3, for coupling with a reference rack either in edge (4a) or middle (4b) position in the row. The added mass at the

reference rack is underlined, thus locating its position in the table. Coupling is found very large between racks, even when belonging to different rows, which is related to the relatively small gaps between opaque structures (a similar situation is encountered in fast breeder reactors, for the canned fuel assemblies). Coupling with the pool walls is notably smaller, because of the larger gaps around the rack array, yet remains essential for an appropriate description of the overall in-phase motion. The rack-to-wall coupling values are not very dependent upon rack position, as it could be expected from the general interpretation of coupling with the containment in section 2.

Table 4 : Geometrical representation of coupling coefficients with a given rack.

<u>18.74</u>	- 13.79	- 1.84	- 6.57	(4a)
8.36	- 4.45	- 1.46	(walls)	
- 13.79	<u>30.10</u>	- 13.79	- 5.75	(4b)
- 4.44	11.09	- 4.44	(walls)	

The cross-directional (XY) coupling is not intrinsically negligible, with a maximum value equal to 8.2. But the sum of the terms for a rack is zero, because this coupling has no influence in the rigid-body motion of the whole system. From symmetry considerations, this remains valid in the in-phase motion of the rack array (with negligible off-centering), or for a standard inner position of a rack in a larger array. The elimination of such a coupling is not of much importance, except perhaps for very local effects.

6.3. Remarks on practical determination and application

Many structural models comprise a rack single row (Champomier et al. 1989, Shah et al. 1994). As for fuel assemblies, the direct input of the previous values is not consistent : the sum of terms in the first rows of tables 4a and 4b, including the wall division, is equal to -3.46 or -3.23 instead of -1. Assuming identical row motions leads to the addition of the terms in the same table column (i.e. lump with out-of-row coupling) but the resulting increase in coupling terms may be found arbitrary. An alternative method is to perform a correction on the computed values (except for wall coupling), relatively weak with respect to the large values, and also required when limiting coupling to neighbouring racks. For larger arrays, the case of inner and outer rows should be distinguished. Structural models of the complete rack array are more favourable for coupling consistency, but with a complex configuration of the node-to-node coupling elements; a direct input of the total added mass matrix is certainly preferable, as when coupling is defined for deformable structures.

Allowance for the fluid vertical motion from the very large three-dimensional f.e. models is hardly feasible, and an approximate correction is acceptable. For preserving the benefit of f.e. determinations, a semi-analytical method can be envisaged : Fourier series represent the dependence on vertical position, which leads to one plane f.e. solution per included term.

7. NON-LINEAR EFFECTS

The linear character of hydrodynamic coupling is related to the hypothesis of small motion amplitudes, then leading to a negligible convective term in momentum equation (2). The general form of non-linear coupling can be derived from Lagrange equations, with an added mass matrix depending on displacements in the fluid kinetic energy. Hence the hydrodynamic force corresponding to the i th. structural degree of freedom is :

$$f_i = - \sum_{j=1}^n m_{ij} \ddot{x}_j - \sum_{j,k=1}^n a_{ijk} \dot{x}_j \dot{x}_k \quad (9)$$
$$a_{ijk} = \frac{\partial m_{ik}}{\partial x_j} - \frac{1}{2} \frac{\partial m_{jk}}{\partial x_i}$$

where the dependence of added mass coefficients on the instantaneous geometrical configuration also implies the existence of the (non-dissipative) quadratic velocity terms.

The amplitudes of the fuel assembly lateral motions can reach values exceeding the fuel rod diameter, with resulting flows and dissipative drags, but hydrodynamic coupling is concerned only with the configuration of the rod rigid array surroundings. The influence of the configuration change is negligible with lateral confinement, since coupling is independent of the axial gaps. For the actual in-core configuration, the change in lateral gaps is more significant, but its influence is likely to have the same order of magnitude as the neglected coupling between assemblies, and to be negligible in the key coupling with baffles. Linearity is therefore consistent and justified with the basic model.

Non-linear phenomena occur in the fluid layers between assembly grids (including dissipative), related to the squeeze film dynamics described by Esmonde et al. (1992). Yet the total height of the grids is relatively small (10 % of assembly), and coupling effects between grids cannot be clearly identified from the seismic tests in section 5.

A significant coupling non-linearity is a priori more obvious in the large coupling between racks, and practical forms of eq. (9) have been established from approximate macroscopic balances by Stabel et al. (1993). The method is attractive, but the coupling influence should be compared with that from linear models, which are easier to handle and also reflect a large response decrease in water. It is believed that the model refinement brought by non-linearity should be balanced with the many approximations in the structural models and in coupling distribution, in a reasonable estimate of the predominant phenomena in seismic response.

8. CONCLUSIONS

Hydrodynamic coupling is characterized by very simple governing equations and representation in structural models, yet this simplicity may be misleading for coupling interpretation and determination. For large sets of immersed structures, the necessary simplifications should lead to a physically consistent behaviour in the limiting cases of in-phase motions, and coupling with the containment is never negligible. For the fuel assembly single row models currently used in seismic analysis, assuming row lateral confinement reduces coupling to that between assembly and core baffles, independent of assembly position. This very simple coupling model is justified from the small coupling between assemblies found with calculations, and from its coherence with the in-

water response decrease observed in seismic tests; the tests also justify the single row model. Then the artificial conservatism of the models comprising a single added mass at assembly is eliminated. The large coupling between fuel storage racks is more complex to analyze and to implement. A careful estimate of the different approximations is recommended, in relationship with the computed or tested seismic response, in order to preclude illusory sophistications in structural or coupling models. It is hoped that apart from practical results, the previous considerations will provide useful guidelines for appropriate modelling of coupling, more especially since complete and accurate experimental validations are hardly feasible.

REFERENCES

- Brochard D., Hammami L., 1991, Non-Linear Seismic Analysis of Nuclear Reactor Cores by an Homogenization Method, PVP Conf., San Diego, Vol. 223.
- Champomier F., Delemontey R., Sollogoub P., Toumbas D., 1989, Seismic Design of a Spent Fuel Storage Rack, SMIRT 10, Anaheim, Vol. K 2.
- Callens C., Leroux J.C., Rigaudeau J., 1991, Status of Methods for Justification of Fuel Assembly Lateral Strength during an Earthquake, SMIRT 11, Tokyo, C 6/1.
- Esmonde H., Fitzpatrick J.A., Rice H.J., Axisa F., 1992, Modelling and Identification of Non-linear Squeeze Film Dynamics, Jour. of Fluids and Structures, 6, 223-248.
- Fritz R.J., 1972, The Effects of Liquids on the Dynamic Motions of Immersed Solids, ASME Jour. of Engin. for Industry, 94, 167-173.
- Jeanpierre F., Gibert R.J., Hoffman A., Livolant M., 1979, Description of a General Method to Compute the Fluid Structure Interaction, SMIRT 5, Berlin.
- Leroux J.C., De Perthuis S., Rigaudeau J., 1993, Qualification of Industrial Models for the Justification of Fuel Assembly Lateral Strength during an Earthquake, SMIRT 12, Stuttgart, K 16/1.
- Levy S., Wilkinson P.D., 1975, Calculation of Added Water Mass Effects for Reactor System Components, SMIRT 3, London, F 2/5.
- Rigaudeau J., Brochard D., Benjedidia A., 1993, Fluid Structure Interaction in the Response of PWR Fuel Assemblies to Horizontal Seismic Loads, SMIRT 12, Stuttgart, K 17/5.
- Queval J.C., Gantenbein F., Rigaudeau J., 1991, Experimental Studies on Seismic Behaviour of PWR Fuel Assembly Rows, PVP Conf., San Diego, Vol. 20.
- Queval J.C., Gantenbein F., De Perthuis S., 1993, Experimental Studies on Seismic Behaviour of PWR Fuel Assemblies, SMIRT 12, Stuttgart, 17/6.
- Scavuzzo R.J., Stokey W.F., Radke E.F., 1979, Dynamic Fluid Structure Coupling of Rectangular Modules in Rectangular Pools, PVP 39, 77-86.
- Shah S.J., Harstead G.A., Kopecky B., 1994, Seismic and Structural Analysis of High Density/Consolidated Spent Fuel Storage Racks, ANS meeting, DOE Spent Nuclear Fuel - Challenges and Initiatives, Sun Valley.
- Stabel J., Ren M., Swelim H., 1993, Calculation of Seismic Loads on Fuel Storage Racks under Consideration of Fluid Structure Interaction, SMIRT 12, Stuttgart, K 15/6.

CASAC Validation Report
[b,c,d]